Biomatter 3:3, e24926; July/August/September 2013; © 2013 Landes Bioscience

Mechanical models for the self-organization of tubular patterns

Chin-Lin Guo

Department of Bioengineering; California Institute of Technology; Pasadena, CA USA

Keywords: mechanics, mechanical force, extracellular matrix, tissues, self-organization, pattern formation, morphogenesis

Organogenesis, such as long tubule self-organization, requires long-range coordination of cell mechanics to arrange cell positions and to remodel the extracellular matrix. While the current mainstream in the field of tissue morphogenesis focuses primarily on genetics and chemical signaling, the influence of cell mechanics on the programming of patterning cues in tissue morphogenesis has not been adequately addressed. Here, we review experimental evidence and propose quantitative mechanical models by which cells can create tubular patterns.

Introduction

Life depends on the ability to control size and shape at different scales. At the molecular levels, chemical signaling relies on the conformational changes of molecules: mutations leading to abnormal changes of conformations often cause diseases such as tumors, tissue abnormality and malfunction. At the cellular level, the ability of cells to form various shapes has a vital importance.[1,2] Such ability appears to control the fate of cells, including cell apoptosis,[3] direct cell migration,[4] and cell differentiation.[5] At the tissue levels, the ability of cells to self-organize into various structures with a long-range coordination of their morphologies and phenotypes raises the possibility that an understanding of such processes could lead to a synthetic approach to engineer and/or regenerate tissue-scale structures and even organs without the aid of scaffolds.

The most abundant tissue structures that exhibit long-range coordination of cell morphologies and phenotypes are epithelial tubules, which appear in the respiratory, reproductive, digestive, and renal systems, and can be up to several centimeters long.[6-9] In the past decades, theoretical studies have suggested that long-range morphological patterns can be created by chemical reaction-diffusion, and extensive experimental studies have been performed to investigate how chemical signals are involved in tubule formation in vivo.[9-13] Nevertheless, attempts to create tissue-scale tubular structures by chemical stimulations in vitro have seen limited success. Consequently, current engineering of long tubules and other tissue-scale structures still relies on scaffolds,[14,15] which typically require complicated fabrication and must remain with the engineered tissue, limiting their clinical applications.

Besides chemical stimulation, evidence increasingly suggests that extracellular matrix (ECM) plays an important role in tubular pattern formation.[9-12,16] Type I collagen (COL), for example, an ECM molecule that can form long linear fibers, often appears around long tubules in vivo.[17] Cells have also been shown to create long-range linear morphological patterns (up to 600 μm) through mechanical interactions with collagen molecules in vitro.[4] Such interactions require cell surface receptors integrins that link ECM with various intracellular cytoskeletons.[18] In particular, when the matrix environment is changed from laminin-rich (the major ECM component in basement membrane[19]) to collagen-rich, cells can switch integrin-linked cytoskeleton from intermediate filaments to actomyosin, thereby switching their phenotypes from stable epithelial structures to motile cells.[20]

These experimental observations raise the possibility that cells might use mechanical interactions, along with their chemical signals, to create tissue-scale tubular patterns. Indeed, a growing interest has been developed to investigate the roles of mechanical force in tissue development, remodeling, regeneration, and tumorigenesis.[21-25] Understanding how cell mechanics are involved in tubular pattern formation requires familiarity with engineering principles of mechanics, the viscoelastic properties of biomaterials, and the integration of force and stress within tissue-scale structures as morphogenesis progresses. Here, we review experimental evidence and propose quantitative mechanical models by which cells can create the tubular patterns. Our primary focus is to discuss how biomaterials such as ECM can be used to engineer or regenerate tubular patterns—the mechanisms and models proposed here need not to be the ones used or observed in vivo.

Chemical-Based Turing Models for Tubular Pattern Formation

We first briefly discuss the current chemical-based models for tubular pattern formation. Epithelial tubules are either a single long cylindrical structure or a tree-like structure with iterative branches of simple cylindrical units, by which cells can create long-range transport of gas or fluids, and/or maximize the surface area for efficient gas exchange or secretion of fluids across the surfaces. In vivo, branching morphogenesis of tubular organs including lungs,[12,26] blood vessels,[7,26] salivary glands,[27] mammary

Correspondence to: Chin-Lin Guo; Email: guochin@caltech.edu
Submitted: 04/16/13; Revised: 05/03/13; Accepted: 05/03/13
Citation: <insert here>; http://dx.doi.org/10.4161/biom.24926

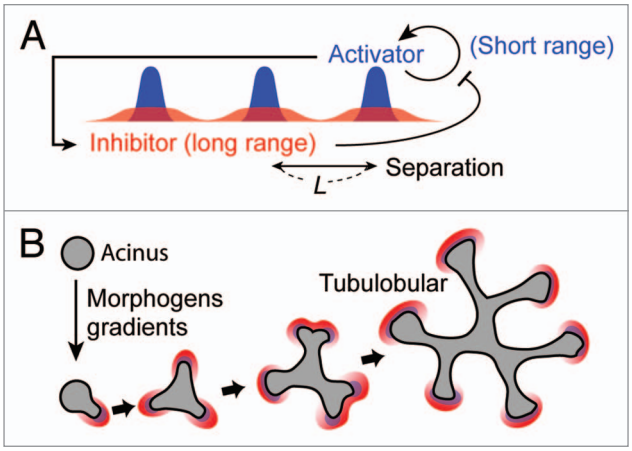

Figure 1. The schematics of chemical-based lateral inhibition. (**A**) Lateral inhibition requires a short-range activation that self amplifies and a long-range inhibition that inhibits remote activations. The strength of the stimulation and the spatial characteristics of the activation and the inhibition determine the spacing *L*. (**B**) Hypothetical tubular pattern formed by chemical reaction-diffusion (blue: activator, red: inhibitor, gray: cells).

glands,[26] and renal ducts[8,26,28] involves an reiterative branching of cells from pre-existing cell sheets to the surrounding ECM.[7,26] Similar processes can be found in embryo gastrulation, where a group of cells from ectoderm bend inward to form endoderm.[29]

To create tubular patterns, the two important parameters are the spatial scale and the geometry of the tubules. One appealing mechanism to create repetitive tubular pattern is the chemical reaction-diffusion scheme proposed by Alan Turing (lateral inhibition).[13] Lateral inhibition relies on the interplay of short-range activation and long-range inhibition (**Fig. 1**). Such inhibition can result from the consumption of precursors or the creation of inhibitors. Lateral inhibition requires that the activation self amplifies, while creating inhibition to suppress other activations. As a result, individual activations mutually repel each other, leading to a regular spacing, *L*, between neighboring activations. In turn, position cues can spontaneously emerge to pattern cells into regular/periodic structures.

While chemical patterning has been observed in simple chemical systems and developmental processes,[30] there is no successful example to create tubular patterns and other tissue-scale patterns by chemical stimulations in vitro.[31] The main difficulty arises from the extensive remodeling of ECM and the substantial movements of cells during tissue self-organization and morphogenesis, which could significantly interference with the chemical patterning processes.[32] Further, in the presence of other cells such as mesenchymal cells, the environment surrounding epithelial cells becomes more complex, and the secretion, degradation, and distribution of diffusible chemical factors become less predictable.

Mechanics-Based Non-Turing Models for Tubular Pattern Formation

General features of mechanical forces in pattern formation. In chemical-based lateral inhibition, the formation of spatial patterns requires that the activation and the inhibition possess different spatial scales; this is achieved by having activators and inhibitors with different diffusion constants.[12,26,28,33-39] Further, to form robust spatial patterns in complex and fluctuating environments, it is necessary that the spatial scales of activators and inhibitors possess a certain degree of flexibility. The diffusion constants of bio-molecules, however, are usually not tunable, limiting the dynamic range of tissue pattern formation by chemical-based processes.

Compared with chemical-based patterning processes, several features of mechanical forces make them easier to create spatial patterns. One feature is the tunability of cell motility, which makes it possible to create a broad range of spatial scales. Consider two types of cells that interact with each other. These cells can create different motilities by tuning their cytoskeletal mechanics and/or the expression level of surface receptors that mediate cell-cell or cell-ECM adhesions. Assume that the slow-moving cells act as the activator and the fast-moving cells act as the inhibitor. We can then see how their interactions lead to lateral inhibition. Examples can be found in the patterning of skin appendages, such as hair follicles[34] and feather buds,[40] where mesenchymal cells interact with epithelium and change motility by expressing different amounts of receptor N-CAM. Such cell motion-based lateral inhibition is also applicable to the cases where a single type of cells switch their phenotypes in response to an inhibitor released by the cells (such as transforming growth factor[41]). In these cases, the difference of spatial scales is established by the diffusion of the inhibitor and the tunability of the cell motility.

Another feature that makes mechanical force useful in patterning processes is its vectorial nature. Such feature allows information of mechanical forces to be delivered in the same direction over a long spatial range in a short amount of time. This effect reduces the dispersion and/or dissipation of information, a common consequence in chemical diffusion. Further, the vectorial nature of mechanical forces creates spatial anisotropy. Consider a mechanical process that involves two forces transmitted along two orthogonal axes. These forces can be generated by moving cells along the ECM fibers. In contrast to isotropic molecular diffusion, the magnitude of each force lasts for a long spatial range along its own principle axis, but limited in the other. This effect leads to a difference of spatial scales for the distribution/dispersion of forces between orthogonal axes, a feature that cannot be achieved by simple chemical diffusion.

Perhaps the most important feature of mechanical forces is that they can continuously propagate between and across cells through cytoskeletons, intercellular adhesions,[42,43] and ECM.[25] This feature provides long-range and instant communication within the tissue-scale structures. The instant propagation of forces over multiple cells can be used to mimic the long-range effect required for chemical-based lateral inhibition. Further, patterning cues mediated by mechanical force can propagate among cells and ECM without the transformation of the patterning information by biochemical cues, such as morphogens. Unlike chemical signals, however, mechanical forces are not specific and cannot be amplified. Thus, the coupling of mechanical forces and chemical signals is necessary for robust pattern formation.

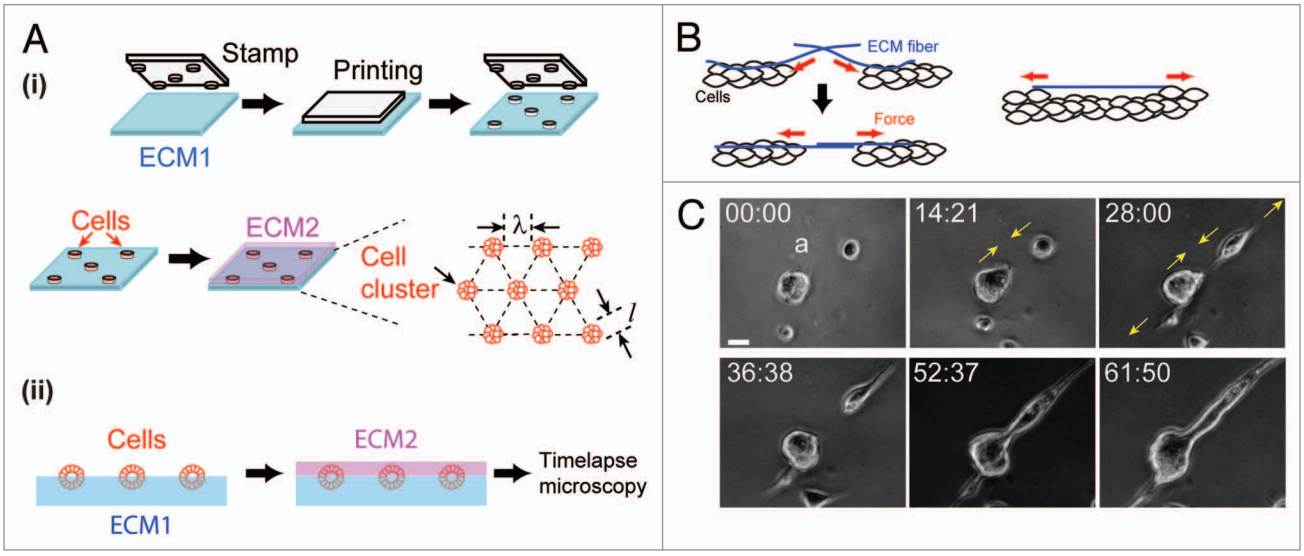

Figure 2. Mechanical interaction leads to long-range linear morphological patterns. (**A**) Schematics of the setup for the measurement of mechanical interactions among groups of cells. (**i**) The size of cell group (*l*) and the distance between groups (λ) can be controlled by micro-patterning. (**ii**) The 2-layer ECM setup enables the study of cell mechanical interactions in response to the change of ECM. (**B**) Schematics to show how mechanical interactions lead to the rearrangement and alignment of ECM fibers (Left), which then allow cells within the tissue to remotely influence each other, thereby creating long-range coordination (Right). (**C**) Example of linear pattern formation by mechanical interactions, adapted from reference.[4] Epithelial cells were grown into acini in laminin-rich matrix environment for two days and the matrix was switched to collagen-rich matrix at t = 00:00. Cells switched morphologies into linear patterns by developing long-range mechanical interactions through collagen fibers. Time is in hours and minutes. Scale bar: 50 μm.

Tension and spatial scales created by mechanical processes. Several models have been proposed to address how mechanical forces and remodeling of ECM can facilitate branching morphogenesis in tubular organs.[44-46] It was suggested, for example, that cells can degrade ECM at the nascent branching sites, while strengthening ECM at the non-branching sites, thereby creating branching patterns as the 'fingering' process in viscous media.[44-46] These models, however, do not provide any quantitative mechanisms for how the two important parameters in tubular pattern formation, i.e., the spatial scale and the geometry, can spontaneously emerge through mechanical or mechano-chemical processes in cell-cell and cell-ECM interactions.

From a theoretical point of view, the control of molecular conformation, cell shape, tissue morphology, and ECM architecture relies on how mechanical forces are created, distributed, and transmitted. In most cases, mechanical force is transmitted by filaments such as actomyosin bundles inside the cells and extracellular matrix (ECM) fibers outside the cells. The spatial scales of these filaments range from micrometers to the size of organs. At the cellular level, the creation of force within single cells depends on the orientation and distribution of actomyosin filaments, while the propagation of forces between cells depends on cell-cell contacts. At the tissue level, the propagation of force within tissues is parameterized by the orientation and distribution of ECM molecules.

If cells can use mechanical forces to program tubular patterns, one immediate question is how far cells can develop mechanical interactions with one another. Certainly, the spatial scales of such interactions are parameterized by the architecture of the environments. Measuring these scales requires a quantitative platform. Owing to the advanced technologies of micro-patterning, several groups have engineered platforms to study how mechanical stress within the tissues depends on the geometry of tissue boundaries, how far cells can mechanically sense each other through ECM, and how cells change their phenotypes in response to the change of ECM.[4,47,48] On the boundaries of tissue, for example, it has been shown that the effects of mechanical forces between cells are determined by the curvature of the boundaries.[46] Likewise, it was observed that cells can mechanically sense each other at a sub-millimeter scale, and through mechanical interactions, cells can collectively change their phenotypes by translocating molecules such as Yes-associated protein (YAP), a signaling molecule for mechano-transduction,[49] into the nuclei.[4]

Figure 2A shows an example of such platforms, by which one can measure how groups of cells change their patterns of mechanical interactions in response to the changes of ECM and how far they can interact with one another. Remarkably, it was found that cells can mechanically interact with each other through collagen fibers over a distance ~600 μm, which is far beyond the persistence length of collagen fibers and the typical diffusion length created by molecular diffusion (~10–20 μm).[4] The tension created by the cells along the collagen fibers then facilitates the formation of long-range linear cellular patterns (**Fig. 2B and C**).[4] In particular, the traction forces created by individual cells help the alignment of collagen fibers, which then confine cell motions.[4] Such behavior can be used as a foundation to create long linear tubules.

Branching patterns emerging from mechanical processes. We now discuss how cells could use tension on the cell-matrix interface, i.e., the boundaries of tissues (**Fig. 2B**), and other

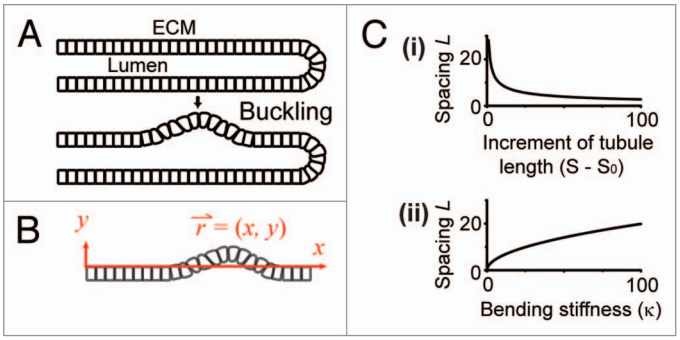

Figure 3. Branching patterning due to a buckling effect. (**A**) The schematics of the buckling effect. (**B**) The schematics of the coordinates for the modeling of tubular surface topology. (**C**) Predictions of the model. The spacing between branched sites, *L*, (**i**) decreases with the increment of cell number, $S - S_0$, and (**ii**) increases with the bending stiffness, *k*. Results were obtained using Equation 6 with $S_0 = 100$ and $\sigma = 1$. In (**i**), $\kappa = 100$. In (**ii**), $S = 120$.

chemical-based cell regulations (such as cell proliferation, switch of phenotypes, and tuning of cell motility) to program spatial patterns. We propose and discuss the following models.

Formation of branching patterns by a buckling effect. One possible effect of the tension on the cell-ECM interface is to create a bending stiffness that helps cells align linearly with the collagen fibers. This effect can suppress the surface roughness of the tubules. In the presence of growth factors such as epidermal growth factor which stimulates cell proliferation,[50] however, the tubule cannot carry excessive cells without changing its surface topology or its length. As a result, the cells will be bended into the lumen or the ECM space (i.e., buckling) if the length is confined. A spatial pattern then emerges by the mechanical balance between the bending stiffness and the proliferation pressure (**Fig. 3A**). Using a Helfrich energy function,[51] Mark et al. have introduced a bending stiffness-based mechanical model to address dynamic instability in an expanding cell sheet.[52] Here, we discuss how cell proliferation and the bending stiffness at the cell-ECM interfaces can give rise to branching patterns.

Consider a flat cell-ECM interface on the boundary of a linear tubule (**Fig. 3B**). For simplicity, we use a 1-D topology to represent the surface of the tubule. The surface area is then the integral of arc length of the tubule. The length of the tubule is confined as S_0 by the surrounding matrix environment. After a certain amount of time, the number of cells increases and the proliferation pressure pushes the tubule to reach a new equilibrium length *S*, which is not allowed due to the confinement, leading to the formation of buckles (i.e., bending cells into the matrix, **Fig. 3A**).

To analyze branching pattern formation, let's use coordinate $\vec{r} = (x, y)$ to describe the surface of the tubule (initial $y = 0$ everywhere on the tubule surface). Adapting the equations from reference 52 the simplest 2-D free energy function *F* that takes into account both the bending energy and the confinement of tubule length is:

$$F = \frac{\kappa}{2}\int_{x=0}^{x=S_0} ds\left(\frac{d^2\vec{r}}{ds^2}\right)^2 + \frac{\sigma}{2}\left[\int_{x=0}^{x=S_0} ds - S\right]^2. \quad (1)$$

Here, κ is the bending stiffness, σ is the intracellular pressure to push the extension of the tubule, and $ds = (dx^2 + dy^2)^{1/2}$ is the arc length along the tubule surface. Following the variation procedure introduced in reference 52, we can perform a variation of *F* with respect to the coordinates $\vec{r}$, which gives the equation of motion of $\vec{r}$:

$$\eta\frac{d\vec{r}}{dt} = -\frac{\delta F}{\delta \vec{r}}. \quad (2)$$

Here, η is the viscosity of the tubule surface when cells move into the ECM space. To investigate how branching patterns emerge on the tubule surface, consider a small perturbation of the tubule surface, i.e., $y << S_0$. Expanding **Eqn. 2** to the first order of *y*, we have:

$$\eta\frac{dy}{dt} = -\kappa\frac{d^4y}{dx^4} - \sigma\left[S - S_0\right]\frac{d^2y}{dx^2} + O(y^2). \quad (3)$$

Using mode analysis with $y(k) = y_0(k)\exp[\omega(k)t]$ where *k* is the wavenumber, we have a dispersion relation:

$$\eta\omega(k) = -\kappa k^4 + \sigma\left[S - S_0\right]k^2. \quad (4)$$

Eqn. 4 indicates that the tubule surface is marginally stable. It also predicts that instability occurs (i.e., $\omega(k) > 0$) when $S > S_0$. The wavenumber with the maximal growth rate, k_{max}, and the corresponding spacing between branched sites, *L*, are:

$$k_{\max} = \sqrt{\frac{\sigma\left[S - S_0\right]}{2\kappa}}, \quad (5)$$

$$L = \frac{2\pi}{k_{\max}} = \frac{2\pi\sqrt{2\kappa}}{\sqrt{\sigma\left[S - S_0\right]}}. \quad (6)$$

This model predicts that the spacing between branched sites along the tubule surface, *L*, decreases with the increment of cell number [**Fig. 3C** (**i**)], which is controlled by the dosage of growth factors, while *L* increases with the bending stiffness (i.e., the tension at cell-ECM interface) [**Fig. 3C** (**ii**)].

Branching pattern formation by surface tension and cell scattering. Besides bending stiffness, another possible effect due to the tension on the cell-ECM interface is to minimize the surface area of epithelial tubules and to confine the motion of cells on the surface. To investigate how such effect can lead to branching pattern formation, consider a group of cells that escape or scatter from a preexisting tubule surface into the surrounding ECM (**Fig. 4A**). In vivo and In vitro, such scattering can be induced by stimulating cells with scattering factors such as hepatocyte growth

factor.[53] As more cells scatter into the ECM, the local curvature and the local surface area of the tubule increase (**Fig. 4A**). These scattering cells can interact with the ECM and create force to 'pull' even more cells to scatter outward. Further, the pulling force is in a direction orthogonal to the tension (i.e., spatial anisotropy due to the vectorial nature of mechanical force, **Fig. 4B**), leading to a 'local' effect to convert more non-scattering cells into the scattering cells. Localization of such conversion effect can be destroyed if the scattering cells move along the tubule surface (i.e., lateral diffusion).

Based on these arguments, we assume that the rate at which the scattering cells are created is enhanced by the local convexity of the tubule surface and suppressed by the lateral movement of scattering cells along the tubule surface. In the absence of chemical stimulations, branching patterns might spontaneously emerge due to a mechanical counterbalance between the scattering and the tension: while the tension globally minimizes the surface area and suppresses the surface convexity, the scattering effect locally amplifies the surface convexity.

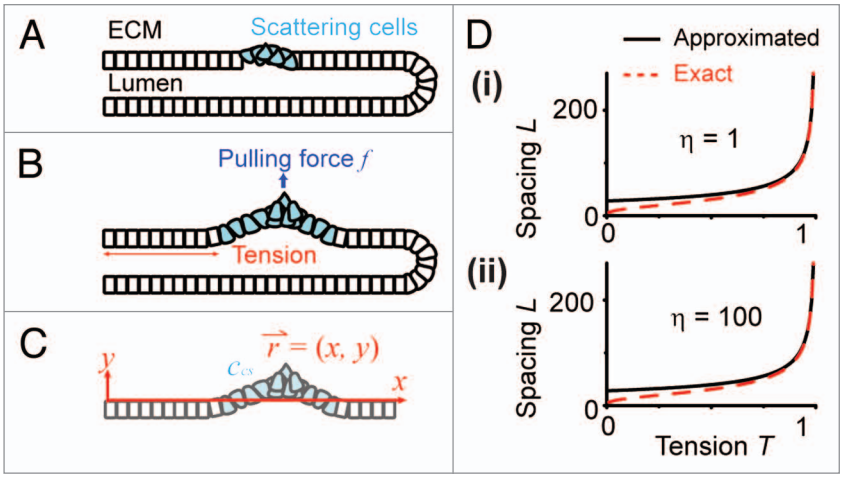

Figure 4. Branching pattern formation due to surface tension and cell scattering. (**A**) The schematics of cell scattering (cyan) from a tubule surface, by which the local curvature (i.e., convexity) of tubule surface increases. (**B**) The scattering cells create force (blue arrow) to drag or pull more cells outward, in a direction perpendicular to the tension. (**C**) The schematics of the coordinates for the modeling of tubular surface topology. c_{cs} is the local density of scattering cells. (**D**) Numerical results for the approximated solution (**Eqn. 15**), black, and the exact solution (**Eqn. 17**), red, of the spacing L in response to the change of tension T. The viscosity η is set as 1 in (**i**), and 100 in (**ii**). To obtain the results, we set $g = 1$, $f' = 1$, $G' = 1$, and $D_c = 10$ in **Eqns. 15 and 17**.

To investigate whether branching patterns can spontaneously emerge in the absence of chemical stimulations, consider the cross-section of a cylindrical tubule along its tubule axis (**Fig. 4C**). For simplicity, we again use a 1-D contour to represent the surface of the tubule with $\vec{r} = (x, y)$ as the surface coordinate. The surface area is the integral of arc length of the tubule. Following **Eqn. 1**, we write a simple free energy function F to describe the minimization of tubule surface area:

$$F = T\int_{x=0}^{x=S_0} ds. \tag{7}$$

Here, S_0 is the initial length (i.e., surface area in 1-D topology) of the tubule, T is the tension that minimizes the surface area, and $ds = (dx^2 + dy^2)^{1/2}$ is the arc length along the tubule surface. Variation of F with respect to the coordinates $\vec{r}$ gives the equation of motion of $\vec{r}$:

$$\eta\frac{d\vec{r}}{dt} = -\frac{\delta F}{\delta \vec{r}} + \vec{f}(c_{sc}). \tag{8}$$

Here, η is the viscosity of the tubule surface when cells move into the ECM. We add a new term $\vec{f}$, which is the traction force created by the scattering cells to pull the surface outward. This traction force is a function of the local density of scattering cells, c_{sc}, which we assume to increase at a rate proportional to the local convexity of the surface:

$$\frac{dc_{cs}}{dt} = G(-\frac{d^2\vec{r}}{ds^2}\cdot\hat{y}) - gc_{cs} + D_c\nabla^2 c_{cs}. \tag{9}$$

Here, the first term describes the local curvature-dependent increment rate of scattering cells. To ensure that the rate is positive when the surface forms a local convex curvature, we multiply the curvature term with the unit vector of y. The second term describes the conversion of scattering cells back to non-scattering cells and/or the escape of scattering cells into the ECM. The third term describes the diffusion of scattering cells along the tubule surface. Comparing **Eqns. 8 and 9**, the characteristic time scale for scattering cell formation is g^{-1}, while the characteristic time scale for the morphological change of tubule surface (i.e., branching formation) is η.

To investigate how branching patterns emerge on the tubule surface, consider a small perturbation of the tubule surface, i.e., $y << S_0$ and $c_{sc} << 1$. Expanding **Eqn. 8** to the first order of y and c_{sc}, we have:

$$\eta\frac{dy}{dt} = T\frac{d^2y}{dx^2} + f'(0)c_{cs} + O(y^2, c_{cs}^2). \tag{10}$$

Here, $f'(0)$ is the derivative of f with respect to c_{sc} (at $c_{sc} = 0$), and we set $f(0) = 0$ since it is the force created by scattering cells. Likewise, expanding **Eqn. 9** to the first order of y and c_{sc}, we have:

$$\frac{dc_{cs}}{dt} = -G'(0)\frac{d^2y}{dx^2} - gc_{cs} + D_c\frac{d^2c_{cs}}{dx^2} + O(y^2, c_{cs}^2). \tag{11}$$

Here, $G'(0)$ is the derivative of G with respect to the curvature (at zero curvature), and we set $G(0) = 0$ (i.e., no spontaneous

scattering on flat tubule surface in the absence of chemical stimulations).

Branching pattern formation by separation of time scales. We now consider two different conditions where cells can create branching patterns. In the first, we assume that the dynamics of scattering cell formation is much faster than the morphological change of the tubule surface, i.e., $g >> \eta^{-1}$, which is likely the case in a 3-D matrix environment that prohibits cell movement. Under this condition, we can solve **Eqn. 11** adiabatically and express c_{sc} in terms of y using iterative substitution:

$$c_{cs} \approx -\frac{G'(0)}{g}\frac{d^2y}{dx^2} + \frac{D_c}{g}\frac{d^2c_{cs}}{dx^2} \approx -G'(0)\left[\frac{d^2y}{gdx^2} + D_c\frac{d^4y}{g^2dx^4}\right]. \quad (12)$$

Substituting **Eqn. 12** into **Eqn. 10**, we have:

$$\eta\frac{dy}{dt} \approx \left[T - \frac{f'G'}{g}\right]\frac{d^2y}{dx^2} - \frac{D_c f'G'}{g^2}\frac{d^4y}{dx^4}. \quad (13)$$

Using mode analysis with $y(k) = y_0(k)\exp[\omega(k)t]$ where k is the wavenumber, we have a dispersion relation:

$$\eta\omega\left(k^2\right) \approx -\left[T - \frac{f'G'}{g}\right]k^2 - \frac{D_c f'G'}{g^2}k^4. \quad (14)$$

Here, we have simplified the notions of f' and G'. Compared with **Eqn. 4**, **Eqn. 14** also suggests that the tubule surface is marginally stable. However, in **Eqn. 4** the dissipation effect is due to the bending stiffness k, whereas in **Eqn. 14** the dissipation results from the lateral movement of scattering cells along the tubule surface, D_c. Instability occurs when $Tg < f'G'$. Under such condition, the wavenumber with the maximal growth rate is obtained by solving $d\omega(k^2)/dk^2 = 0$:

$$k_{\max} = \sqrt{\frac{g}{2D_c}\left(1 - \frac{Tg}{f'G'}\right)}. \quad (15)$$

This approximated result suggests that the spacing between branched sites along the tubule increases with the motility of scattering cells along the tubule surface and the tension at the cell-ECM interface, while it requires a critical collective effect to amplify the scattering cell density (parameterized by the term G') and overcome the tension and the conversion (and/or escape) of scattering cells (parameterized by g).

Branching pattern formation without separation of time scales. In the second condition, we assume that the time scale in scattering cell formation is compatible with the time scale in morphological change of the tubule surface, i.e., $g \sim \eta^{-1}$, which can occur if the scattering cells are actively secrete enzymes to degrade the surrounding matrix. Under this condition, we cannot use the adiabatic approximation (i.e., **Eqn. 12**). Instead, we have to perform mode analysis with $c_{sc}(k) = c_0(k)\exp[\omega(k)t]$ and $y(k) = y_0(k)\exp[\omega(k)t]$ on **Eqns. 10 and 11**, to obtain the dispersion relation:

$$\eta\omega^2(k^2) + \left[\eta(g + D_c k^2) + Tk^2\right]\omega(k^2) + Tk^2\left(g + D_c k^2 - \frac{G'f'}{T}\right) = 0. \quad (16)$$

Compared with **Eqns. 4 and 14**, **Eqn. 16** also suggests that the tubule surface is marginally stable. Similar to **Eqn. 14**. Instability occurs when $Tg < f'G'$. The wavenumber with the maximal growth rate is then obtained by solving $d\omega(k^2)/dk^2 = 0$:

$$k_{\max} = \sqrt{\frac{g}{D_c}\left(\frac{\sqrt{A_1^2 + A_2A_0} - A_1}{A_2}\right)}, \quad \text{with (17)}$$

$$A_0 = \left(\frac{f'G'}{g\eta D_c} + 1\right)\left(\frac{f'G'}{Tg} - 1\right),$$

$$A_1 = \frac{2f'G'}{g\eta D_c} + 1 - \frac{T}{\eta D_c},$$

$$A_2 = \left(1 - \frac{T}{\eta D_c}\right)^2.$$

Comparing the numerical results from **Eqns. (15) and (17)**, we find that the approximated solutions (**Eqn. (15)**) for the spacing asymptotically reach the exact solutions (**Eqn. (17)**) in the high tension region, regardless of the viscosity η (**Fig. 4D**).

Conclusion

In this article, we discuss how mechanical forces propagating along biomaterials such as ECM can create tension to facilitate long-range coordination of cell morphology and phenotype, and propose quantitative models to address how branching patterns can spontaneously emerge by the counterbalance between tension and other mechano-chemical based processes. We also provide quantitative predictions that can be tested by experiments. The effect of mechanical force on biological materials differs from that of chemical force in that it depends both on the force-molecular interactions and the structure of underlying substrate. This opens a door for using biomaterials and cell mechanics to control and/or engineer tissue-scale structures by changing the topology and structure of the environment. Further, the difference of time scales in force propagation and chemical signaling

enables future engineering and control of patterning cues by combining synthetic biology and the fabrication/manipulation of biomaterials.

There are several advantages of using physical vs. chemical forces to control the response of biological materials. For example, mechanical force is nonspecific, which does not depend on the type of molecules, cells, and tissues involved. Thus, the effect and design principle is universal. Further, unlike specific chemical signaling, the non-specificity of mechanical forces allows them to be directly combined, providing a simple computation law for the programming of mechanics-based patterning processes. These features, along with the relatively simple processes required in generating mechanical processes, make mechanical force a promising tool to control and manipulate tissue morphologies.

Disclosure of Potential Conflicts of Interest

The authors declare that they have no competing interests.

Acknowledgments

The author acknowledges Ellison Medical Foundation and Western Heavens Fund for the support.

References

1. Lecuit T, Lenne PF. Cell surface mechanics and the control of cell shape, tissue patterns and morphogenesis. Nat Rev Mol Cell Biol 2007; 8:633-44; PMID:17643125; http://dx.doi.org/10.1038/nrm2222.
2. Settleman J, Baum B. Cell shape and tissue morphogenesis. Semin Cell Dev Biol 2008; 19:213-4; PMID:18316214; http://dx.doi.org/10.1016/j.semcdb.2008.02.002.
3. Chen CS, Mrksich M, Huang S, Whitesides GM, Ingber DE. Geometric control of cell life and death. Science 1997; 276:1425-8; PMID:9162012; http://dx.doi.org/10.1126/science.276.5317.1425.
4. Grosberg A, Kuo PL, Guo CL, Geisse NA, Bray MA, Adams WJ, et al. Self-organization of muscle cell structure and function. PLoS Comput Biol 2011; 7:e1001088; PMID:21390276; http://dx.doi.org/10.1371/journal.pcbi.1001088.
5. Horowitz A, Murakami M, Gao Y, Simons M. Phosphatidylinositol-4,5-bisphosphate mediates the interaction of syndecan-4 with protein kinase C. Biochemistry 1999; 38:15871-7; PMID:10625452; http://dx.doi.org/10.1021/bi991363i.
6. Martin-Belmonte F, Mostov K. Regulation of cell polarity during epithelial morphogenesis. Curr Opin Cell Biol 2008; 20:227-34; PMID:18282696; http://dx.doi.org/10.1016/j.ceb.2008.01.001.
7. Horowitz A, Simons M. Branching morphogenesis. Circ Res 2008; 103:784-95; PMID:18845818; http://dx.doi.org/10.1161/CIRCRESAHA.108.181818.
8. Shah MM, Sampogna RV, Sakurai H, Bush KT, Nigam SK. Branching morphogenesis and kidney disease. Development 2004; 131:1449-62; PMID:15023929; http://dx.doi.org/10.1242/dev.01089.
9. Warburton D, Schwarz M, Tefft D, Flores-Delgado G, Anderson KD, Cardoso WV. The molecular basis of lung morphogenesis. Mech Dev 2000; 92:55-81; PMID:10704888; http://dx.doi.org/10.1016/S0925-4773(99)00325-1.
10. Bellusci S, Furuta Y, Rush MG, Henderson R, Winnier G, Hogan BL. Involvement of Sonic hedgehog (Shh) in mouse embryonic lung growth and morphogenesis. Development 1997; 124:53-63; PMID:9006067.
11. Bellusci S, Grindley J, Emoto H, Itoh N, Hogan BL. Fibroblast growth factor 10 (FGF10) and branching morphogenesis in the embryonic mouse lung. Development 1997; 124:4867-78; PMID:9428423.
12. Chuang PT, McMahon AP. Branching morphogenesis of the lung: new molecular insights into an old problem. Trends Cell Biol 2003; 13:86-91; PMID:12559759; http://dx.doi.org/10.1016/S0962-8924(02)00031-4.
13. Turing A. The chemical basis of morphogenesis. Philos Trans R Soc Lond B Biol Sci 1952; 237:37; http://dx.doi.org/10.1098/rstb.1952.0012.
14. Grafton MM, Wang L, Vidi PA, Leary J, Lelièvre SA. Breast on-a-chip: mimicry of the channeling system of the breast for development of theranostics. Integr Biol (Camb) 2011; 3:451-9; PMID:21234506; http://dx.doi.org/10.1039/c0ib00132e.
15. Mori H, Gjorevski N, Inman JL, Bissell MJ, Nelson CM. Self-organization of engineered epithelial tubules by differential cellular motility. Proc Natl Acad Sci U S A 2009; 106:14890-5; PMID:19706461; http://dx.doi.org/10.1073/pnas.0901269106.
16. Ito M, Yang Z, Andl T, Cui C, Kim N, Millar SE, et al. Wnt-dependent de novo hair follicle regeneration in adult mouse skin after wounding. Nature 2007; 447:316-20; PMID:17507982; http://dx.doi.org/10.1038/nature05766.
17. Hinck L, Silberstein GB. Key stages in mammary gland development: the mammary end bud as a motile organ. Breast Cancer Res 2005; 7:245-51; PMID:16280048; http://dx.doi.org/10.1186/bcr1331.
18. Giancotti FG, Ruoslahti E. Integrin signaling. Science 1999; 285:1028-32; PMID:10446041; http://dx.doi.org/10.1126/science.285.5430.1028.
19. Kalluri R. Basement membranes: structure, assembly and role in tumour angiogenesis. Nat Rev Cancer 2003; 3:422-33; PMID:12778132; http://dx.doi.org/10.1038/nrc1094.
20. Rabinovitz I, Mercurio AM. The integrin alpha-6beta4 functions in carcinoma cell migration on laminin-1 by mediating the formation and stabilization of actin-containing motility structures. J Cell Biol 1997; 139:1873-84; PMID:9412479; http://dx.doi.org/10.1083/jcb.139.7.1873.
21. Miron-Mendoza M, Seemann J, Grinnell F. Collagen fibril flow and tissue translocation coupled to fibroblast migration in 3D collagen matrices. Mol Biol Cell 2008; 19:2051-8; PMID:18321993; http://dx.doi.org/10.1091/mbc.E07-09-0930.
22. Ingber DE. Mechanical control of tissue morphogenesis during embryological development. Int J Dev Biol 2006; 50:255-66; PMID:16479493; http://dx.doi.org/10.1387/ijdb.052044di.
23. Huang S, Ingber DE. Cell tension, matrix mechanics, and cancer development. Cancer Cell 2005; 8:175-6; PMID:16169461; http://dx.doi.org/10.1016/j.ccr.2005.08.009.
24. Yeung T, Georges PC, Flanagan LA, Marg B, Ortiz M, Funaki M, et al. Effects of substrate stiffness on cell morphology, cytoskeletal structure, and adhesion. Cell Motil Cytoskeleton 2005; 60:24-34; PMID:15573414; http://dx.doi.org/10.1002/cm.20041.
25. Paszek MJ, Zahir N, Johnson KR, Lakins JN, Rozenberg GI, Gefen A, et al. Tensional homeostasis and the malignant phenotype. Cancer Cell 2005; 8:241-54; PMID:16169468; http://dx.doi.org/10.1016/j.ccr.2005.08.010.
26. Affolter M, Zeller R, Caussinus E. Tissue remodelling through branching morphogenesis. Nat Rev Mol Cell Biol 2009; 10:831-42; PMID:19888266; http://dx.doi.org/10.1038/nrm2797.
27. Patel VN, Rebustini IT, Hoffman MP. Salivary gland branching morphogenesis. Differentiation 2006; 74:349-64; PMID:16916374; http://dx.doi.org/10.1111/j.1432-0436.2006.00088.x.
28. Costantini F, Kopan R. Patterning a complex organ: branching morphogenesis and nephron segmentation in kidney development. Dev Cell 2010; 18:698-712; PMID:20493806; http://dx.doi.org/10.1016/j.devcel.2010.04.008.
29. Keller R, Davidson LA, Shook DR. How we are shaped: the biomechanics of gastrulation. Differentiation 2003; 71:171-205; PMID:12694202; http://dx.doi.org/10.1046/j.1432-0436.2003.710301.x.
30. Kicheva A, Cohen M, Briscoe J. Developmental pattern formation: insights from physics and biology. Science 2012; 338:210-2; PMID:23066071; http://dx.doi.org/10.1126/science.1225182.
31. Wei C, Larsen M, Hoffman MP, Yamada KM. Self-organization and branching morphogenesis of primary salivary epithelial cells. Tissue Eng 2007; 13:721-35; PMID:17341161; http://dx.doi.org/10.1089/ten.2006.0123.
32. Hsu JC, Yamada KM. Salivary gland branching morphogenesis--recent progress and future opportunities. Int J Oral Sci 2010; 2:117-26; PMID:21125789; http://dx.doi.org/10.4248/IJOS10042.
33. Jung HS, Francis-West PH, Widelitz RB, Jiang TX, Ting-Berreth S, Tickle C, et al. Local inhibitory action of BMPs and their relationships with activators in feather formation: implications for periodic patterning. Dev Biol 1998; 196:11-23; PMID:9527877; http://dx.doi.org/10.1006/dbio.1998.8850.
34. Sick S, Reinker S, Timmer J, Schlake T. WNT and DKK determine hair follicle spacing through a reaction-diffusion mechanism. Science 2006; 314:1447-50; PMID:17082421; http://dx.doi.org/10.1126/science.1130088.
35. Zegers MM, O'Brien LE, Yu W, Datta A, Mostov KE. Epithelial polarity and tubulogenesis in vitro. Trends Cell Biol 2003; 13:169-76; PMID:12667754; http://dx.doi.org/10.1016/S0962-8924(03)00036-9.
36. Comer FI, Parent CA. Phosphoinositides specify polarity during epithelial organ development. Cell 2007; 128:239-40; PMID:17254962; http://dx.doi.org/10.1016/j.cell.2007.01.010.
37. Nishio M, Watanabe K, Sasaki J, Taya C, Takasuga S, Iizuka R, et al. Control of cell polarity and motility by the PtdIns(3,4,5)P3 phosphatase SHIP1. Nat Cell Biol 2007; 9:36-44; PMID:17173042; http://dx.doi.org/10.1038/ncb1515.
38. Horowitz A, Simons M. Branching morphogenesis. Circ Res 2009; 104:e21; PMID:19179661; http://dx.doi.org/10.1161/CIRCRESAHA.108.191494.
39. Bridgewater D, Rosenblum ND. Stimulatory and inhibitory signaling molecules that regulate renal branching morphogenesis. Pediatr Nephrol 2009; 24:1611-9; PMID:19083023; http://dx.doi.org/10.1007/s00467-008-1048-y.
40. Jiang TX, Jung HS, Widelitz RB, Chuong CM. Self-organization of periodic patterns by dissociated feather mesenchymal cells and the regulation of size, number and spacing of primordia. Development 1999; 126:4997-5009; PMID:10529418.

41. Daniel CW, Silberstein GB, Van Horn K, Strickland P, Robinson S. TGF-beta 1-induced inhibition of mouse mammary ductal growth: developmental specificity and characterization. Dev Biol 1989; 135:20-30; PMID:2767334; http://dx.doi.org/10.1016/0012-1606(89)90154-1.
42. Ragsdale GK, Phelps J, Luby-Phelps K. Viscoelastic response of fibroblasts to tension transmitted through adherens junctions. Biophys J 1997; 73:2798-808; PMID:9370474; http://dx.doi.org/10.1016/S0006-3495(97)78309-7.
43. Vaezi A, Bauer C, Vasioukhin V, Fuchs E. Actin cable dynamics and Rho/Rock orchestrate a polarized cytoskeletal architecture in the early steps of assembling a stratified epithelium. Dev Cell 2002; 3:367-81; PMID:12361600; http://dx.doi.org/10.1016/S1534-5807(02)00259-9.
44. Moore KA, Polte T, Huang S, Shi B, Alsberg E, Sunday ME, et al. Control of basement membrane remodeling and epithelial branching morphogenesis in embryonic lung by Rho and cytoskeletal tension. Dev Dyn 2005; 232:268-81; PMID:15614768; http://dx.doi.org/10.1002/dvdy.20237.
45. Gjorevski N, Nelson CM. Branch formation during organ development. Wiley Interdiscip Rev Syst Biol Med 2010; 2:734-41; PMID:20890968; http://dx.doi.org/10.1002/wsbm.96.
46. Gjorevski N, Nelson CM. The mechanics of development: Models and methods for tissue morphogenesis. Birth Defects Res C Embryo Today 2010; 90:193-202; PMID:20860059; http://dx.doi.org/10.1002/bdrc.20185.
47. Nelson CM, Vanduijn MM, Inman JL, Fletcher DA, Bissell MJ. Tissue geometry determines sites of mammary branching morphogenesis in organotypic cultures. Science 2006; 314:298-300; PMID:17038622; http://dx.doi.org/10.1126/science.1131000.
48. Gjorevski N, Nelson CM. Endogenous patterns of mechanical stress are required for branching morphogenesis. Integr Biol (Camb) 2010; 2:424-34; PMID:20717570; http://dx.doi.org/10.1039/c0ib00040j.
49. Dupont S, Morsut L, Aragona M, Enzo E, Giulitti S, Cordenonsi M, et al. Role of YAP/TAZ in mechanotransduction. Nature 2011; 474:179-83; PMID:21654799; http://dx.doi.org/10.1038/nature10137.
50. Coleman S, Silberstein GB, Daniel CW. Ductal morphogenesis in the mouse mammary gland: evidence supporting a role for epidermal growth factor. Dev Biol 1988; 127:304-15; PMID:3259938; http://dx.doi.org/10.1016/0012-1606(88)90317-X.
51. Safran SA. Statistical thermodynamics of surfaces, interfaces, and membrane. Bounlder, CO: Westview Press, 2003.
52. Poirier MG, Eroglu S, Marko JF. The bending rigidity of mitotic chromosomes. Mol Biol Cell 2002; 13:2170-9; PMID:12058078.
53. Ikari T, Hiraki A, Seki K, Sugiura T, Matsumoto K, Shirasuna K. Involvement of hepatocyte growth factor in branching morphogenesis of murine salivary gland. Dev Dyn 2003; 228:173-84; PMID:14517989; http://dx.doi.org/10.1002/dvdy.10377.